Available online at www.sciencedirect.com

ScienceDirect

Journal of the European Ceramic Society 27 (2007) 2317–2323

www.elsevier.com/locate/jeurceramsoc

EAFD-loaded vitreous and glass–ceramic materials

P. Kavouras[a], Th.A. Ioannidis[b], Th. Kehagias[a,*], I. Tsilika[a],
K. Chrissafis[a], S. Kokkou[a], A. Zouboulis[b], Th. Karakostas[a]

[a] Physics Department, Aristotle University, 541 24 Thessaloniki, Greece
[b] Department of Chemistry, Aristotle University, 541 24 Thessaloniki, Greece

Received 11 March 2006; received in revised form 19 July 2006; accepted 28 July 2006
Available online 22 September 2006

Abstract

SiO_2, Na_2O and CaO were mixed and co-melted with electric arc furnace dust waste. The resulting vitreous materials, produced by quenching at ambient atmosphere, were transformed into glass–ceramics by two-stage heat treatment, under thermal conditions that were determined by differential thermal analysis. X-ray diffraction, scanning electron microscopy, energy dispersive spectrometry and transmission electron microscopy were employed to investigate the physical properties of all products. It was found that whilst wollastonite ($CaSiO_3$) separates from the parent matrix as the dominant crystalline phase in all glass–ceramic products, the crystallization mode depends on the batch composition. Leaching tests evidenced that vitreous products were chemically durable. Devitrification did not significantly affect leach resistance so glass–ceramic materials retain the leach resistance that was achieved by vitrification.

Keyword: Glass ceramics; Microstructure-final; X-ray methods; Optical microscopy; Waste stabilization

1. Introduction

Electric arc furnace dust (EAFD) poses as one of the most intensely growing waste streams on a global scale. This stems from the continuously raising portion in the overall steel production that steel scrap recycling facilities posses. Namely, steel scrap recycling facilities fabricated one-third of the global steel production in 1998, while it is estimated that the world production will reach 5 million tonnes in 2005. In Greece all five steel factories are scrap-recycling facilities, where a total amount of 15,000 tonnes of EAFD is produced annually. Such significant quantities are due to the fact that for every ton of recycled steel an amount of 15–20 kg of EAFD is produced.

EAFD is characterized as a hazardous solid waste according to the United States Environmental Protection Agency (USEPA) classification: it contains significant quantities of lead in the form of lead oxide (PbO), iron and zinc compounds in the forms of zinc oxide (ZnO) and zinc ferrite ($ZnFe_2O_4$). EAFD is produced from the volatilization of heavy metals when steel scrap is melted in the electric arc furnace. Volatilized metals are oxidized and subsequently solidified and detained in the form of fine powder in specially designed filters, which are placed in the electric arc furnace gas stream cleaning system.

In most cases, the part of metallic Zn that is found in ZnO is recovered from the EAFD by hydrometallurgical or pyrometallurgical processes. Nevertheless, the resulting residue is still a hazardous solid waste in powder form, since it is Zn- and Pb-loaded. It is thus essential to develop an additional process that stabilizes the residue of Zn recovery processes. One of the most promising methods is vitrification with the addition of batch materials.[1,2] This arises from the fact that the focus of research has shifted from the mere inertization of toxic wastes to their use in a production cycle.[3] Vitrification, except from a well-established stabilization technique, is a method for the production of vitreous[4] or glass–ceramic materials,[5] which can be used for construction or decorative applications.[6]

In the present study, the vitrification method was used for the production of inert vitreous materials. Subsequently, thermal treatment was applied to transform vitreous products into glass–ceramics. The batch materials mixed with EAFD powder were silica (SiO_2), sodium (Na_2O) and calcium (CaO) oxides. The morphology of vitreous and glass–ceramic products was inspected with optical microscopy and scanning electron microscopy (SEM), whereas their elemental composition

---

[*] Corresponding author. Tel.: +30 2310 998023; fax: +30 2310 998589.
E-mail address: kehagias@auth.gr (Th. Kehagias).

0955-2219/$ – see front matter © 2006 Elsevier Ltd. All rights reserved.
doi:10.1016/j.jeurceramsoc.2006.07.021

and dispersion was studied by energy dispersive spectrometry (EDS). The crystal structure was investigated by X-ray diffraction (XRD) analysis and the microstructure with transmission electron microscopy (TEM). The DIN[7] and TCLP[8] leaching tests were utilized to evaluate the chemical toxicity of the solid wastes, while the vitreous and glass–ceramic products were tested by the TCLP method and selected samples were also examined with the DIN method.

The need for the implementation of such a variety of characterization methods has been imposed from the very nature of the vitrification and devitrification process products. Namely, they are multicomponent, reactive and, the latter, multiphase materials. In such systems, various types of inhomogeneities can occur in different observation levels, with interacting influences on the physical characteristics of the final products. It is, thus, important to have the more integrated knowledge possible on the properties of the products. Under such conditions we can use the overarching framework of glass science for the interpretation of our results, in a more efficient way.

2. Experimental

The elemental composition of the EAFD waste was investigated with EDS method. Analysis was made on samples that were obtained from a 5 kg powder mass of mechanically homogenised and refined EAFD waste. Mechanical treatment was performed using a Fritsch "Pulverisette O" vibrating frame ball milling apparatus. EDS analysis was performed by an OXFORD ISIS-300 spectrometer attached on a JEOL JSM-840A scanning electron microscope. All analyses were made on 10 disk-shaped green state compacts of 3 cm in diameter.

EAFD powder was mixed with SiO_2, Na_2O and CaO powders and formed three different batch compositions. The solid mixtures were placed in a Pt crucible and they were heated in an LHT 02/18 Nabertherm electric furnace at ambient atmosphere at 1400 °C for 2 h. The melts were poured on stainless steel plates and were rapidly cooled down at room temperature. As-quenched products were pulverized and different particle size fractions were obtained. They were characterized by differential thermal analysis (DTA) in order to obtain: (a) the glass transition temperature (T_g); (b) the position of exothermic peaks that would presumably correspond to crystal phase separation; (c) the influence of the particle size (i.e. sample's specific area) on the position of the maximum of the exothermic peak (T_{max}). DTA scans were obtained with a Setaram TG–DTA SetSys 1750 °C instrument in Argon atmosphere. Heating and cooling rates were set at 10 °C/min and the samples were placed in Al_2O_3 crucibles.

A two-stage isothermal treatment process was applied to all as-quenched products. In the first isothermal stage, nucleation takes place and in the second crystal growth occurs. The duration of these two stages were fixed at 15 min for the nucleation and 30 min for the crystal growth process. The nucleation stage was placed 200 °C below exothermic peaks maxima, namely at 680 °C, while crystal growth stage was placed a few degrees above them, at 900 °C.

All as-quenched and annealed products were morphologically characterized by optical microscopy, using a Zeiss Axiolab-A microscope, and SEM. Structural characterization was performed by XRD analysis with a Seifert 3003 powder diffractometer, using Cu Kα1 radiation. TEM was employed for microscopic inspection of the initial products. Specimens for TEM were thinned by mechanical grinding, followed by ion-milling to reach electron transparency. TEM observations were carried out in a JEOL 2010 electron microscope, operated at 200 kV.

The chemical toxicity of EAFD waste was determined by the DIN and TCLP standard leaching test, while all vitreous and glass–ceramic samples were tested by the TCLP standard leaching test and selected samples were also examined by the DIN method to examine certain other important parameters, such as the pH and specific conductivity. The leachates were analyzed to determine their metal content and certain other ions such as sodium, calcium and silicon were also measured.

3. Results

3.1. EAFD composition

The chemical composition of the homogenised EAFD powder mass is shown in Table 1. EAFD powder was heated up to 1000 °C to determine the loss-on-ignition (LOI) mass. Zinc and iron were found to be the main constituents, in accordance with previous similar studies.[9] XRD observations revealed that iron and zinc are found in zinc oxide and zinc ferrite crystalline compounds. The corresponding XRD diagram is presented in Fig. 1, where the high intensity peaks correspond to $ZnFe_2O_4$ and ZnO, while some lower intensity peaks correspond to PbO.

The application of DIN and TCLP standard-leaching tests proved that the examined EAFD can be classified as a hazardous waste according to the maximum permissible limits of both applied methods as presented in Table 2. Iron and chromium

Table 1
Composition (wt.%) of EAFD powder in oxide compounds

MgO	0.7
Al_2O_3	0.9
SiO_2	4.1
K_2O	1.4
CaO	4.6
MnO	3.3
Fe_2O_3	33.9
ZnO	34.9
PbO	6.2
LOI	7.8
Humidity	2.0

Table 2
Leaching tests results, performed on the mechanically homogenized EAFD waste

Leaching method	pH	Zn	Pb	Cd
DIN	11.83 ± 0.05	0.8 ± 0.01	29 ± 5	ND[a]
TCLP	6.63 ± 0.05	371 ± 7.00	44.8 ± 0.3	5.40 ± 0.07

Concentrations of metals measured in the leachates are expressed in mg/l.
[a] Not detected, i.e. Cd content <0.4 mg/l.

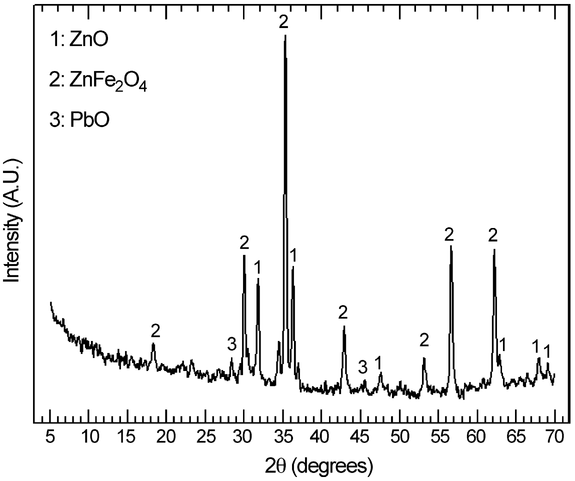

Fig. 1. X-ray diffractogram of the pulverized and homogenized EAFD waste.

Table 3
Batch compositions (wt.%) with the silicon over oxygen and sodium over calcium atomic ratios

	EAFD	SiO_2	Na_2O	CaO	Si/O	Na/Ca
EAFD1	20	55	10	15	0.359	0.90
EAFD2	20	55	5	20	0.360	0.45
EAFD3	15	55	5	25	0.362	0.35

were not found in the leachates whereas manganese concentrations were also measured in the area 3–5 mg/l. The pH values of the resulting leachates proved that the alkali and/or alkali metal release would be relatively high when the EAFD comes in contact with aqueous solutions.

3.2. Vitrification products

Batch compositions for vitrification are listed in Table 3, together with the Si/O and Na/Ca atomic ratios. The former ratio is a measure of the connectivity of the silica-based vitreous network[10] and the latter is related to the ability for long-range diffusion of Na and Ca ions.[11,12] The selection of the specific oxide powders that were mixed with EAFD waste was based on the fact that they are found in abundance in some non-toxic wastes and natural raw materials, like marble dust, glass cullets, or sand. This is the reason for the relatively low concentration in EAFD in the batch composition of Table 3. For large-scale production the above materials will be used instead of the pure oxides that were used in this study for laboratory scale vitrification.

EDS analyses showed that all elements were homogeneously dispersed into the vitreous matrix, since the standard deviations of elemental compositions did not exceed ±2 at.% that is in the order of the sensitivity of the EDS method. The as-quenched products were X-ray amorphous, as it was confirmed by XRD analysis. The amorphous state is retained down to the microscopic level, since TEM micrographs showed featureless matrices in all initial products, characteristic of homogeneous materials, whereas the corresponding electron diffraction patterns composed of a bright diffuse halo depicting the amorphous nature of the vitreous matrices.

3.3. Devitrification products

The conditions for thermal treatment were designated from the DTA thermographs by defining the position of the exothermic peak that apparently corresponds to crystal phase separation. Three DTA thermographs, each one for different powder particle fraction, were obtained for all vitreous products. Specifically, fine medium and coarse-grained fraction contained powder particle sizes less than 63 μm, between 160 and 250 μm and higher than 0.5 mm, respectively. This investigation was undertaken in order to define the devitrification mode, namely surface or bulk crystallization, which leads to crystal phase separation. It is well known that when the crystallization exothermic peaks shift towards higher temperatures as the mean particle size decreases, the devitrification mode is surface nucleation. In contrast, when their position remains roughly the same the main devitrification mechanism is bulk crystallization. All DTA thermographs are presented in Fig. 2.

From EAFD1 to EAFD3 products, T_g is shifting to higher temperatures, while the temperature interval between T_g and T_{max} ($T_{max} - T_g$) becomes smaller. Additionally, the temperature interval $T_{max} - T_g$, for the same compositions, becomes narrower when we shift from coarse grained towards fine-grained powder particle fractions, as it is shown in Table 4.

It should be pointed out that the DTA experiments were made in inert atmosphere, while all thermal treatments were made in

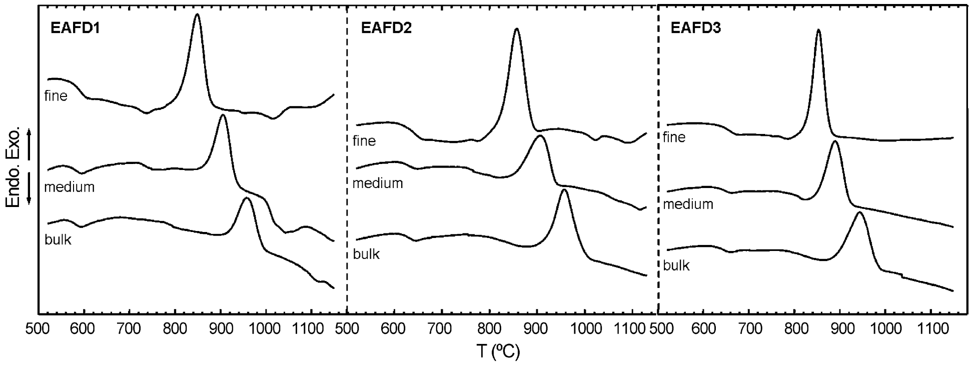

Fig. 2. DTA thermographs of all vitreous products, corresponding to three distinct powder particle size fractions.

Table 4
Position of the glass transition temperatures and exothermic peak maxima and corresponding temperature intervals between the above features, as obtained from the DTA thermographs (temperatures in °C)

	T_g	T_{max} (bulk)	T_{max} (medium)	T_{max} (fine)	$T_{max} - T_g$ (bulk)	$T_{max} - T_g$ (medium)	$T_{max} - T_g$ (fine)	$T_{max}^{bulk} - T_{max}^{fine}$
EAFD1	580	960	905	850	380	325	270	110
EAFD2	620	960	905	860	340	285	240	100
EAFD3	635	945	895	855	310	260	220	90

air. This might raise an argument on whether DTA experiments can be used in order to define thermal treatment conditions. A surface oxidation would possibly affect the shape of the DTA trace, and this would be more pronounced for finely grained products, since they possess a relatively larger specific area. A DTA run was made for finely grained EAFD3 product in air; the two corresponding DTA traces were virtually the same; the position of the base of the exothermic peak is the same, while the difference between the maxima is approximately 20 °C. Therefore, it can be assumed that in our case the DTA traces in inert atmosphere can be used for determining the conditions of thermal treatment in air.

The morphology of the devitrified products is schematically presented in Fig. 3. EAFD1 is composed of a surface opaque devitrified layer, where needle-like crystallites are normally oriented with respect to the surface, and a central transparent amorphous region. EAFD2 and EAFD3 products were composed of the same surface crystallized layer, as EAFD1. The difference was that the central region was crystallized with homogeneously dispersed crystallites with sizes that varied between 2 and 8 μm. For the same thermal conditions, the surface layer in the EAFD2 product was wider with respect to the EAFD3 product. XRD analysis of the devitrified products revealed that in all cases the *wollastonite* ($CaSiO_3$) crystalline phase was separated from the amorphous matrix of the initial products. Both surface devitrified layers and central crystalline regions contain wollastonite crystals. EAFD1 devitrified product shows a more pronounced amorphous bump (Fig. 4) with respect to EAFD2 and EAFD3, i.e. it possesses the smallest degree of crystallinity.

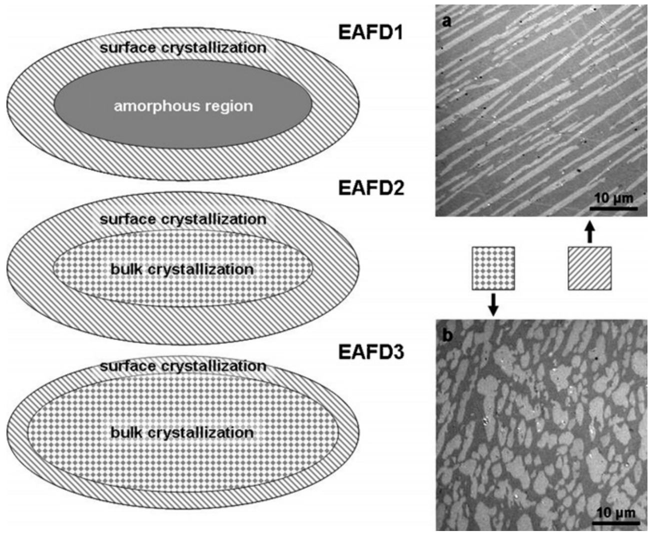

Fig. 3. Schematic representation of the macroscopic cross-section views from all devitrified products (left) that gives a rough estimation of the distribution of the surface and bulk crystallized areas. The corresponding optical micrographs from the two distinct representative areas are also presented (right).

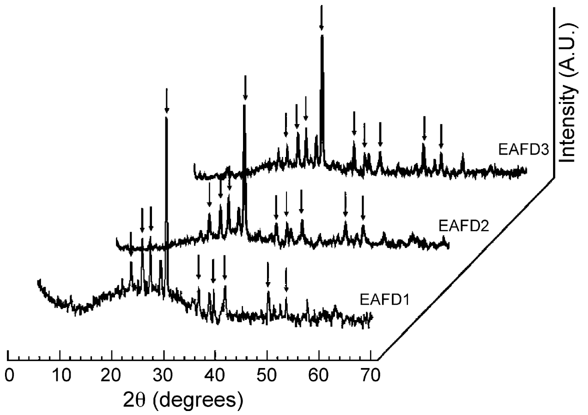

Fig. 4. XRD diagrams of the thermally treated products. Small arrows denote the peaks corresponding to the wollastonite phase.

3.4. Leaching tests

The measured concentrations of the toxic pollutants found in leachates after the application of TCLP method applied to the glass and glass–ceramic materials are presented in Table 5. As it is shown, lead and zinc concentrations in leachates were very low. Similar values have been also recorded in the literature.[13,14] The application of standard leaching tests to the vitrified products revealed that the total release of constituents would be particularly low, especially when de-ionized water is used as leaching solution, such as in the DIN 38414 method. The specific electrical conductivity values measured in the leachates verified the latter. The experimental values after the application of DIN 38414 were below 11 μS/cm, for all samples, indicating that

Table 5
Measured concentrations of heavy metals after the application of TCLP method, performed on vitreous and devitrified products

Sample	Zn (mg/l)	Pb (mg/l)	Cd
As-quenched, vitreous			
EAFD1	0.55	0.24	ND
EAFD2	0.23	0.36	ND
EAFD3	0.20	0.14	ND
Annealed, glass–ceramic			
EAFD1	0.16	0.23	ND
EAFD2	0.20	0.14	ND
EAFD3	0.15	0.14	ND

Not detected, i.e. Cd content <0.4 mg/l.

matrix dissolution would be particularly limited in de-ionized water.

The measurements of the alkali and alkali earth metals supported the previous measurements, as all values were found in the milligram per liter (or below) region. After applying the DIN 38414 method, sodium and calcium concentrations were 0.95, 0.36, 0.45, 0.54 mg/l and 1.54, 0.94, 0.73, 1.03 mg/l for the EAFD1–EAFD3 (glass) and EAFD3 (glass–ceramic) samples, respectively, whereas the molecular ratio of Na^+/Ca^{2+} (in (mmol/l)/(mmol/l)) measured in the resulting leachates varied between 0.67 and 1.07. The obtained pH values were 7, 7.11, 7.34 and 6.95; these values were in accordance with the aforementioned measured concentrations of the alkali and alkali earth metals and suggest that the buffering capacity of the resulting leachates would be particularly limited. Silicon concentrations in leachates were below 0.5 mg/l with the exception of EAFD2 glass sample where the value was 1.32 mg/l when TCLP was used as leaching solution.

4. Discussion

4.1. Vitreous products

The constituent zinc, iron and lead oxides of EAFD powder were homogeneously dispersed in the vitreous matrix of initial products. This is a basic target when stabilization is intended, since segregation or clustering of toxic elements is avoided. It is also a demonstration that the selected batch compositions were not in the region of a stable or meta-stable miscibility gap that would result in undesirable inhomogeneity, which could potentially deteriorate chemical resistance.[15] Leaching tests verified that all initial products were chemically non-toxic, since the concentrations of zinc, lead and cadmium in the leachate were below the legitimate limits. The fact that EAFD waste was stabilized for the batch compositions shown in Table 3 can be explained by the following arguments.

The concentration of SiO_2 in the batch materials, which is the main glass former, is high enough so that the silicon over oxygen atomic ratio (Si/O) is higher than 0.33 in all initial materials (Table 3). As a result, silica is able to construct by itself an extended three-dimensional vitreous network with high degree of interconnectivity.[11] Additionally, iron and zinc ions have been shown that have the role of glass-forming elements. This was determined by means of X-ray absorption fine structure and X-ray fluorescence studies.[16,17] This is important, since iron and zinc can behave either as glass-forming or glass-modifying species, namely they form intermediate oxides. Being glass formers iron and zinc oxides enhance rather than deteriorate the structural integrity of the vitreous network of the initial products. Additionally, according to the Zachariasen–Warren model of the atomic structure in oxide glasses, glass-forming elements are bonded by stronger covalent bonding with the surrounding oxygen ions than glass-modifying ions. If they were glass modifiers they would be bonded by weaker electrostatic bonds and as a result they would presumably be leached away more easily. Consequently, all batch compositions can be used for the production of stabilized vitreous products. However, their devitrification modes vary from surface nucleation to bulk crystallization, according to the relative proportion between sodium and calcium ions.

4.2. Glass–ceramic products

EAFD1 is less receptive to devitrification than EAFD2 and EAFD3. This can be established by comparing the XRD diagrams (c) and (d) in Fig. 3; in particular, the relative intensity of wollastonite peaks with respect to the amorphous bump in EAFD1 is lower compared to the EAFD2 and EAFD3 diffractograms. This is in accordance with the wider temperature interval between the maximum of the exothermic peak that corresponds to the crystallization peak and the glass transition found in EAFD1, compared to EAFD2 and EAFD3 (Table 4) for all corresponding powder particle fractions. It is widely accepted that a vitreous material with wider temperature interval between T_g and T_{max} presents higher thermal stability than another one with narrower temperature interval.[18]

According to the definition by Strnad,[5] only devitrified EAFD2 and EAFD3 products can be considered as glass–ceramic materials. This is due to their respective morphology. Namely, EAFD1 devitrified product is an inhomogeneous material composed of two well-defined regions: a devitrified surface zone, where the needle-like wollastonite crystallites are oriented normal to the surface and a central amorphous region (Fig. 3). On the other hand, thermal treatment of EAFD2 and EAFD3, with the same conditions, resulted to a macroscopically homogeneous glass–ceramic material made up of a residual amorphous matrix that contain homogeneously dispersed wollastonite crystallites of a few micrometers in size (Fig. 3).

The crystallization mode of EAFD1 product is surface nucleation and subsequent growth of wollastonite needle-like crystallites at the expense of the central amorphous region. This is supported from the final morphology of the product and can be established from the DTA results. The fact that the exothermic peak is shifted towards lower temperatures with decreasing particle size is a strong indication that crystallization in this case is a surface effect. In fact, the shift is more pronounced with respect to the other two compositions.

In the cases of the EAFD2 and EAFD3 products, a surface zone composed of needle-like crystallites still exists but it is less wide in EAFD2, while in the case of EAFD3 product its width does not exceed that of a few tens of microns. The shift of the exotherms in EAFD2 and EAFD3 is apparently caused from the surface crystallization and growth of wollastonite needles. However, the shift of the exotherms decreases as the width of the surface region decreases. It can be assumed that bulk devitrification of the central region occurs simultaneously. The decrease of the surface layer takes place because bulk crystallization acts as a barrier to the growth of wollastonite needles, since the homogeneously dispersed crystallites in the central region is wollastonite as well (Fig. 4). The fact that EAFD3 surface region is narrower with respect to the EAFD2 devitrified product can be attributed to the structure of the initial vitreous products.

It is well known that iron is susceptible to devitrification and can act as a precursor to spontaneous devitrification, when found in high enough concentration.[19] Previous studies on vitrification of solid industrial wastes showed that iron took part in the ceramic phase of the resulting glass–ceramic materials. However, in these cases the concentration of iron oxide was not less than 20 wt.% in the whole batch composition.[20] In the present study, iron does not seem to participate in the devitrification process, since the only separated crystal phase is wollastonite. Regarding the composition of EAFD waste, the concentration of iron oxide in the batch compositions does not exceed 7.5 wt.%, which is rather low and possibly the reason why iron does not contribute to the devitrification process. Moreover, it has been shown for the specific solid waste[17] that the bonding environment of iron remains unaffected by thermal treatment. Specifically, the iron atoms are tetrahedrally coordinated prior and after heat treatment and thus iron behaves as a glass former. As a consequence, iron seems to be more strongly bonded in both vitreous and glass–ceramic matrices and does not take part in the formation of separated crystal phases.

4.3. General comments

The fact that EAFD1 is less receptive to devitrification may be due to the different relative proportion of the two modifying oxides (Na_2O and CaO). It is a well-known phenomenon that each alkali or alkaline earth cation, in the specific case Na and Ca, forms its own connective tissue of diffusion paths inside the primary glass former network. In two extreme cases, where only Na or Ca is present, these paths have the higher degree of percolation and long-range ion diffusion is easier. In the case, where $Ca/Na \rightarrow 1$ the two isolated diffusion paths interpenetrate and disrupt one other and long-range diffusion is constrained. This phenomenon is called the mixed modifier effect (MME), an effect similar to the well-known mixed alkali effect (MAE).[21] MAE is a phenomenon that affects all properties of glasses that depend on long-range motion of ions.[12]

One of the properties strongly affected from MME is crystal growth, since it is connected to reconstructive transformations that are controlled from long-range diffusion of the elements that compose the crystallites. Reconstructive transformations are needed for crystal phase separation, because the composition of the crystal phases is different from that of the parent glass. MME has been used to interpret the durability of nuclear waste glasses.[22] It is reasonable to expect higher tendency of wollastonite separation to EAFD2 and EAFD3 thermally treated products, since in that case the Na^+/Ca^{2+} atomic ratio is 0.45 and 0.30, respectively, while in the case of EAFD1 is 0.90.

5. Conclusions

EAFD powder was mixed with SiO_2, Na_2CO_3 and $CaCO_3$ powders and three batch compositions were prepared for the production of vitreous products. Devitrification occurred by the crystallization of wollastonite from the surface or from the bulk. Initial vitreous and glass–ceramic products, successfully immobilized Zn and Pb, which are the main hazardous elements found in EAFD, as it was found by the application of TCLP leaching test. EAFD2 and EAFD3 batch compositions were found to be the most appropriate for large-scale stabilization of EAFD. They were more easily devitrified and the separated wollastonite crystallites were homogeneously distributed over the whole volume of the sample with similar sizes, except a limited surface area where surface nucleation dominates. This shift in crystallization mode was explained on the basis of the relative proportion between sodium and calcium ions that affects long-range diffusion.

Acknowledgement

This work was co-funded by the European Social Fund and National resources through the EPEAEK II “PYTHAGORAS I” program.

References

1. Colombo, P., Brusatin, G., Bernardo, E. and Scarinci, C., Inertization and reuse of waste materials by vitrification and fabrication of glass-based products. *Curr. Opin. Sol. Stat. Mater. Sci.*, 2003, **7**, 225–239.
2. Bingham, P. A. and Hand, R. J., Vitrification of toxic wastes: a brief review. *Adv. Appl. Ceram.*, 2006, **105**, 21–31.
3. Conner, J. R. and Hoeffner, S. L., A critical review of stabilization/solidification technology. *Crit. Rev. Environ. Sci. Technol.*, 1998, **28**, 397–462.
4. Cambier, F. and Leriche, A., Vitrification. In *Materials Science and Technology Series: Processing of Ceramics-Part II, Volume*, ed. R. J. Brooks. VCH, Weinheim, 1996, pp. 126–127.
5. Strnad, Z., *Glass–Ceramic Materials*. Elsevier, Amsterdam, 1986, pp. 230–234.
6. Hölland, W. and Beall, G., *Glass–Ceramic Technology*. American Ceramic Society, Westerville, 2002, pp. 229–247.
7. Deutsche Norm, German standard methods for the examination of water, waste water and sludge. DIN 38414, 1984.
8. USEPA Test Methods for Evaluating Solid Waste, SW-846. Method 1311, Office of Solid Waste, Washington, DC, 1996.
9. Solifić, T., Rastovčan-Mioč, A., Cerjan-Stefanović, Š., Novosel-Radović, V. and Jenko, M., Characterization of steel mill electric-arc furnace dust. *J. Hazard. Mater. B*, 2004, **109**, 59–70.
10. Shelby, J. E., *Introduction to Glass Science and Technology*. RSC Paperbacks, Cambridge, 1997, pp. 78–86.
11. Day, D., Mixed alkali glasses—their properties and uses. *J. Non-Cryst. Sol.*, 1976, **21**, 343–372.
12. Swenson, J. and Adams, S., Mixed alkali effect in glasses. *Phys. Rev. Lett.*, 2003, **90**, 155507.
13. Pisciella, P., Crisucci, S., Karamanov, A. and Pelino, M., Chemical durability of glasses obtained by vitrification of industrial wastes. *Waste Manage.*, 2001, **21**, 1–9.
14. Pelino, M., Karamanov, A., Pisciella, P., Crisucci, S. and Zonetti, D., Vitrification of electric arc furnace dusts. *Waste Manage.*, 2002, **22**, 945–949.
15. Kavouras, P., Kaimakamis, G., Ioannidis, Th. A., Kehagias, Th., Komninou, Ph., Kokkou, S., Pavlidou, E., Antonopoulos, I., Sofoniou, M., Zouboulis, A., Hadjiantoniou, C. P., Nouet, G., Prakouras, A. and Karakostas, Th., Vitrification of lead-rich solid ashes from incineration of hazardous industrial wastes. *Waste Manage.*, 2003, **23**, 361–371.
16. Pinakidou, F., Katsikini, M., Paloura, E. C., Kavouras, P., Komninou, Ph. and Karakostas, Th., XAFS studies on vitrified industrial waste. *Phys. Scripta T*, 2005, **115**, 931–932.
17. Pinakidou, F., Katsikini, M., Paloura, E. C., Kavouras, P., Kehagias, Th., Komninou, Ph. and Karakostas. Th., On the distribution of bonding environment of Zn and Fe in glasses containing electric arc furnace dust: a μ-XAFS and μ-XRF study. *J. Hazard. Mater.*, 2006, doi:10.1016/j.jhazmat.2006.08.016.
18. Hrubỳ, A., *Czech. J. Phys. B*, 1972, **22**, 1187–1193.

19. Karamanov, A. and Pelino, M., Crystallization phenomena in iron rich glasses. *J. Non-Cryst. Sol.*, 2001, **281**, 139–151.
20. Kavouras, P., Komninou, Ph., Chrissafis, K., Kaimakamis, G., Kokkou, S., Paraskevopoulos, K. and Karakostas, Th., *J. Eur. Ceram. Soc.*, 2003, **23**, 1305–1311.
21. Zarzycki, J., *Glasses and the Vitreous State*. Cambridge University Press, 1990, pp. 309–310.
22. Raman, S. V., The effect of mixed modifiers on nuclear waste glass processing, leaching and Raman spectra. *J. Mater. Res.*, 1998, **13**, 8–15.